JOURNAL OF GEOPHYSICAL RESEARCH, VOL. 106, NO. A2, PAGES 1903–1915, FEBRUARY 1, 2001

# Flow bursts, braking, and Pi2 pulsations

L. Kepko and M. G. Kivelson

Department of Earth and Space Sciences and Institute of Geophysics and Planetary Physics, University of California, Los Angeles, California

K. Yumoto

Department of Earth and Planetary Sciences, Kyushu University, Fukuoka, Japan.

**Abstract.** We examine six near-Earth dipolarization events during which rapid flows were observed by Geotail at distances between 8 and 15 $R_E$ in the magnetotail. Each flow event was associated with local dipolarization, auroral arc brightening, and Pi2 pulsations (periods of 40-150 s). Variations in earthward flow velocity delayed by 60-90 s match the Pi2 waveforms on the ground at low latitudes on the flank. We conclude that low-latitude Pi2 pulsations are directly driven by compressional pulses associated with braking of oscillatory earthward flows. In addition, we identify a new type of nightside Pi2, which is related to the oscillatory braking current that modulates the current in the substorm current wedge. For one event we estimate the magnitude of the braking current from the amplitude of ground perturbations and find $I$~2-3×10$^4$ A. An independent calculation of the inertial current using the flow measurements yields 6×10$^4$ A. We separate Pi2 into three distinct physical types: low-latitude directly driven, nightside transient response, and nightside inertial current. We propose a phenomenological model linking flow bursts, the substorm current wedge, and the three types of Pi2 pulsations.

## 1. Background

It is well known that both Pi2 pulsations ($T$=40-150 s) and fast, convective plasma flows occur near substorm onset (for Pi2, see *Saito* [1969], *Saito et al.* [1976], and *Sakurai and Saito* [1976], and for flows, see, e.g., *Nagai et al.* [1998]). Both phenomena also occur during nonsubstorm conditions, but no direct link between them has been fully established. It is generally argued that flow bursts are linked to Pi2 pulsations in two ways (see review by *Olson* [1999]). The first involves the substorm current wedge, which is generated at substorm onset through a diversion of the cross-tail current [*McPherron et al.*, 1973]. Alfvén waves link this current to the auroral ionosphere, The Alfvén waves are partially reflected because of an impedance mismatch between the ionosphere and magnetosphere [*Maltsev et al.*, 1977; *Mallinckrodt and Carlson*, 1978; *Goertz and Boswell*, 1979; *Nishida*, 1979; *Lysak and Dum*, 1983]. After several bounces, the Alfvén wave dies out. The wave period is determined by the travel time between conjugate ionospheres and is typically ~90-120 s. Ground magnetometers observe a damped sinusoidal waveform, localized to the nightside, with initial amplitudes ~10-20 nT. These are called midlatitude Pi2 and are well described by the transient response model [*Baumjohann and Glassmeier*, 1984; *Southwood and Hughes*, 1985] (see review by *Olson* [1999] for other references).

A second link between flows and Pi2 involves flow deceleration, or braking, that is imposed by the rapidly rising magnetic pressure at the interface between dipolar and stretched tail field lines [*Haerendel*, 1992; *Shiokawa et al.*, 1997]. Though few direct measurements of the braking exist, indirect evidence is abundant. While high-speed flows are frequently seen in the middle magnetotail, they are rarely observed inside of 10 $R_E$, suggesting flow deceleration in that region [*Baumjohann et al.*, 1990; *Angelopoulos et al.*, 1994]. Magnetohydrodynamic (MHD) simulations have also linked the generation of the substorm current wedge to flow braking [e.g., *Birn and Hesse*, 1996]. Midtail plasma flows are observed in the tail a few minutes before the low-latitude Pi2 onset on the ground [*Nagai*, 1998], and these Pi2 are thought to be connected to braking (see, e.g., *Yumoto et al.*, [1989]). Low-latitude Pi2 are just a few nanoteslas in amplitude with periods typically at the low end of the Pi2 period band (~50 s). The frequency of these Pi2 is constant with latitude, and they are sometimes observed on the dayside [*Sutcliffe and Yumoto*, 1989].

The relation between flow braking and low-latitude Pi2 has not been established. It has been suggested that the deceleration of the flow burst serves as a source of broadband power that drives an inner magnetospheric oscillator (such as the plasmasphere). If the compressional signal contains power at the resonant frequency of the oscillator (the cavity), cavity mode pulsations are generated. Many papers have attributed low-latitude Pi2 to cavity mode oscillations in the plasmasphere where standing compressional waves are confined radially by the equatorial ionosphere and the plasmapause [e.g., *Yeoman and Orr*, 1989; *Sutcliffe and Yumoto*, 1991]. However, *Kepko and Kivelson* [1999] have recently suggested that low-latitude Pi2 are directly driven by periodic flow enhancements in the tail and are not driven by a cavity mode.

In this paper, we examine six separate flow burst events observed in the magnetotail to establish the connection between flow bursts, Pi2, and braking. The events are from times when Geotail perigee was located in the nightside plasma sheet between 8 and 15 $R_E$. The events were selected because they followed low levels of geomagnetic activity. We find strong evidence in support of the proposal that low-latitude Pi2 are directly driven and that the periodicity is imposed by periodic flow bursts without the need for an intermediate oscillator [*Kepko and Kivelson*, 1999]. Additionally, we find a new type of Pi2 directly



Paper number 2000JA000158.
0148-0227/01/2000JA000158$09.00

related to transient flow braking. We calculate the inertial current associated with flow deceleration in two independent ways and find good agreement. Finally, we present a phenomenological model unifying flow bursts, braking, the substorm current wedge, and the different types of Pi2 pulsations.

## 2. Events

All six events studied in this paper occurred during a wide range of geomagnetic activity (Figure 1) while Geotail was in the near-Earth magnetotail close to Sun-Earth line (Figure 2). In each event, fast, intermittent plasma flows and magnetic field dipolarization occurred in the span of a few minutes. In addition, each event was associated with auroral arc brightening and ground Pi2 pulsations. Geotail plasma moments are from the low-energy particle (LEP) experiment [*Mukai et al.*, 1994] and the magnetic field data are from the magnetic field (MGF) experiment [*Kokobun et al.*, 1994]. Both provide data at 12-s resolution. In addition, magnetic field data from the 210° mm stations [*Yumoto et al.*, 1996], the Canopus magnetometer array and several other ground stations are used to detect Pi2 pulsations.

### 2.1. September 4, 1997

The event was followed by a rapid 80 nT drop in the *AL* index and ~45 min later by the onset of a large substorm (Figure 1a). Geotail was located at (-9.8, 0.6, 0.1) in GSM coordinates. The positions of the ground stations are shown in Figure 2a. Ewa (Ewa Beach), Dlb (Dalby), and Can (Canberra) were located in the premidnight sector, and their positions have been mapped along dipole field lines to the GSM equatorial (Z=0) plane. The magnetic field and velocity data from Geotail are shown in Figures 3a and 3b. Oscillations in the *X* (earthward) component of the velocity with Pi2 (~1-2 min) periodicity are evident from 0946 to 0953 UT. Several of the bursts also have a negative $V_z$ component. Geotail was located in the southern half of the plasma sheet during the event, and an earthward flow originating in the central plasma sheet would have a southward component as the flow diverged along field lines. During this interval the $B_z$ component of the field increases by ~5 nT. On the basis of Polar VIS and UVI auroral zone images an auroral onset occurred between 0947:12 and 0948:36 UT, which is roughly simultaneous with the start of the flow burst.

Magnetic field data from ground stations are shown Figures 3c and 3d. Oscillations started at the three stations (Ewa, Dlb, and Can) just after 0948 UT. The waveforms of $V_{perpx}$ at Geotail, shifted by +60 s, and the *X* component of the magnetic field measured at Ewa (Figure 3e) are similar over the first three cycles. In particular, the positive *X* and negative *Y* perturbations on the ground at 0949, 0950, and 0951:30 UT are matched by positive $V_{perpx}$ flows at Geotail, as indicated by short, vertical lines. There appears to be a propagation delay from Ewa to Dlb and finally to Can. The flow does not return to zero after the second flow burst, but as we discuss later, it is the relative change

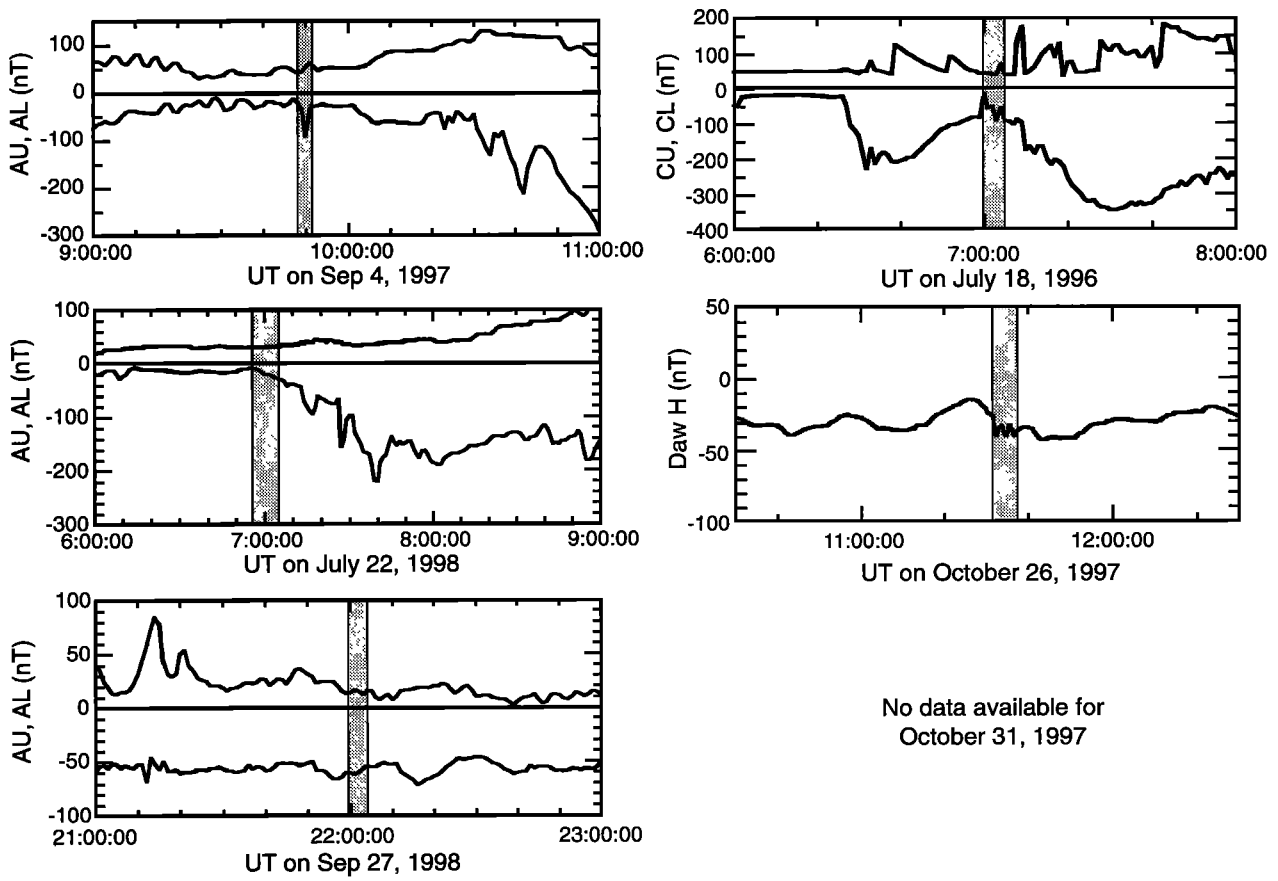


**Figure 1.** Provisional auroral indices for five of the six events in this paper. Gray boxes mark the times that fast flows were observed at Geotail. *CU* and *CL* are plotted for the July 18, 1996, event, and the *H* component from Daw (located near the area of activation) is plotted for the October 26, 1997, event. No auroral data are available for the October 31, 1997, event.

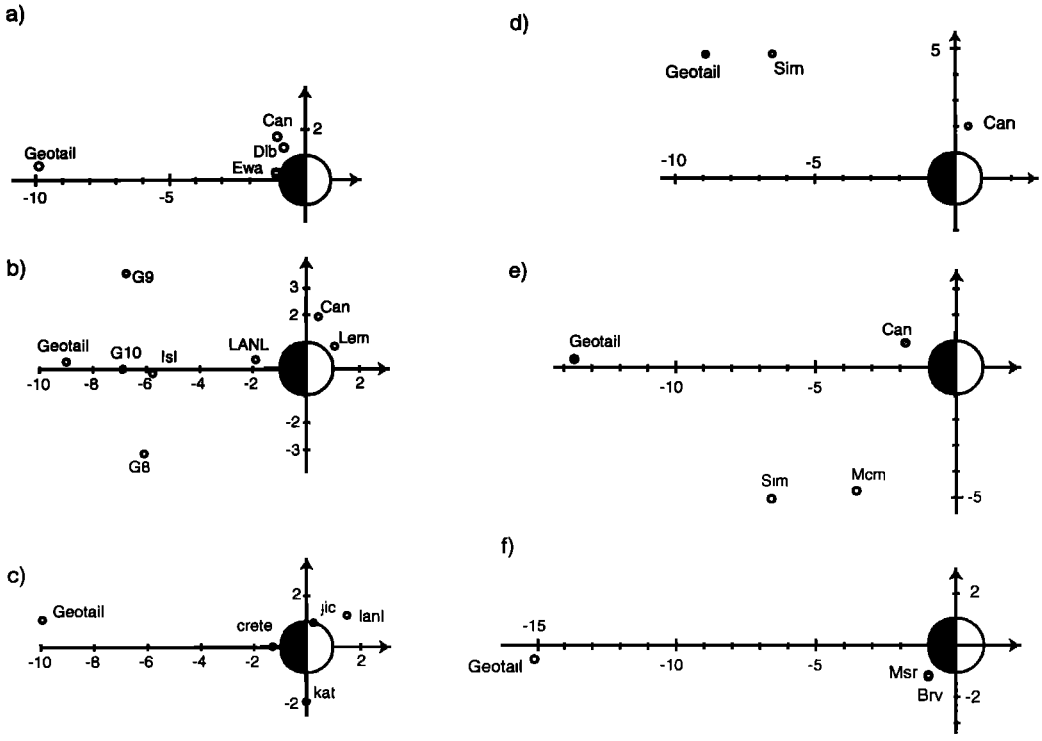


**Figure 2.** GSM locations of the ground stations and Geotail for the six events examined in this paper.

in the flow that is important for coupling to ground oscillations. The change in velocity between the second and third flow burst is ~200 km/s, of the same order as the other flow bursts.

While similar, the flow variations and the ground perturbations do not match exactly. In particular, the third burst seems to require a smaller time shift than the +60 s applied, and the fourth burst at 0952:30 UT (time shifted to 0953:30 UT) is well away from the perturbations near 0953 UT. We will discuss reasons why time shifts may change during an event in section 3.1., but for now we note that the first flow burst at 0947 UT had a large negative (dawnward) $V_y$ component, which directs the flow away from the ground stations. The second and third bursts contained little $V_y$, and a smaller shift of ~50 s would improve agreement with the ground data. The fourth burst, near 0952 UT, contained a large duskward $V_y$ (toward the ground stations), and the +60 s time shift is clearly too large to agree with the $X$ perturbations observed on the ground. Several of the other events will exhibit this characteristic, which suggest that the $V_y$ component may play an important role in determining the appropriate time shift.

### 2.2. July 22, 1998

This event was associated with the onset of a moderate substorm at 0654 UT, with intensifications at 0711 and 0726 UT, and $AL$ reaching a maximum negative value of -200 nT at ~0740 UT (Figure 1b). Geotail was located at (-9.0, 0.3, 0.8) in GSM coordinates. The mapped locations of the ground stations, Geotail, and the positions of the GOES 8, 9, and 10 spacecraft are shown in Figure 2a. As in the previous case, the Geotail velocity data (Figure 4d) show fast, highly variable flow with oscillations in the Pi2 frequency band starting at 0654 UT. $B_z$ increased by almost 20 nT as the magnetic field dipolarized. Polar VIS and UVI images show an auroral onset between 0653:35 and 0658.06 UT. The ground magnetic field data are shown in Figures 4a-4c. Canberra (Can), located on the dayside, observed Pi2 pulsations starting around 0656 UT, mostly in the $X$ component. Island Lake (Isl) and Los Alamos (Lanl), both on the nightside, measured large-scale perturbations associated with a substorm current wedge. Isl, at high latitude, recorded a negative bay while Lanl, at a lower latitude, recorded a positive bay. Each also recorded Pi2 pulsations starting at ~0655:30 UT, with the principal axis of polarization parallel to perturbations arising from the substorm current wedge current. Pi2 pulsations at all ground stations stopped around 0704 UT, near the end of the flow burst. Magnetic field data in spacecraft coordinates from the GOES spacecraft are shown in Figure 5. Pi2 pulsations are evident in all components of the GOES 9 data from 0655 to 0706 UT but are clearly seen only in the $X$ component at GOES 10, despite its location between Geotail and the field line from Island Lake. Local large-amplitude perturbations may obscure the Pi2 pulsations. GOES 8, located farther dawnward, observes a longer-period pulsation not observed by the other GOES spacecraft or any of the ground stations.

The earthward component of the flow velocity and the $X$ component from the Los Alamos (Lanl) magnetometer, located near midnight, are compared in Figure 6. The velocity data from Geotail have been shifted by +60 s, which produces good correlation between individual earthward flow bursts and positive $X$ perturbations measured at Lanl. Similar waveforms were also observed at GOES 9 (Figure 6b), with GOES 9 observing the Pi2 at most a few seconds before Lanl. Finally, the Lanl data are compared to the dayside data from Can and Lem. A +32 s shift produces good correspondence with the negative $X$ fluctuations at Lanl. Several features in the data were considered in identifying what we believe is the correct time shift and polarization. These include the abrupt frequency change at 0704 UT, followed by irregular variations in both records and the bipolar signature after 0711 UT.

Although the temporal variations of the flow velocity and the

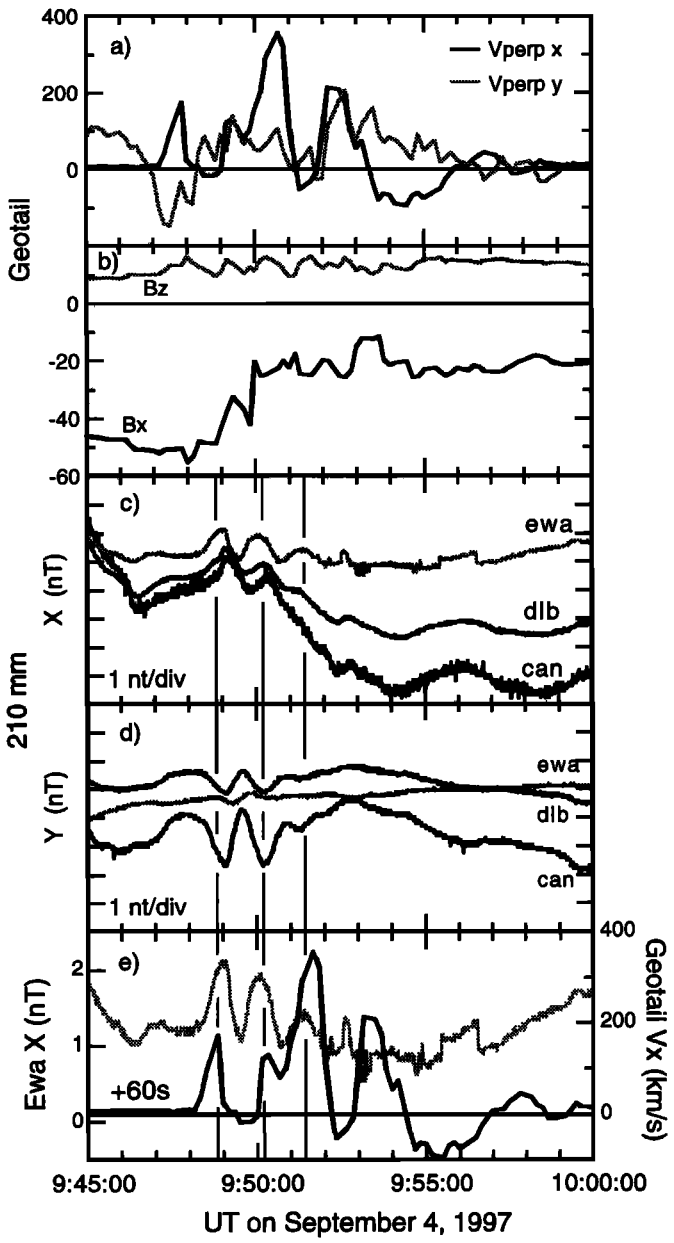


**Figure 3.** Field and particle data from the Geotail spacecraft for the September 4, 1997, event. Plotted are (a) the perpendicular flow velocity in GSE coordinates; (b) $B_x$ and $B_y$ in GSM coordinates; the (c) $X$ and (d) $Y$ components from the Ewa, Dlb, and Can magnetic observatories; and (e) the $X$ component of the perpendicular flow velocity measured at Geotail, shifted by +60 s, and the $X$ component from Ewa. Vertical lines mark the times where variations in the flow velocity match Pi2 waveforms on the ground.

ground Pi2 signatures are similar over the course of the event, the amplitude of the flow variations becomes small while the Pi2 amplitude remains relatively constant. Geotail was located in a region of strong dipolarization after the first few flow bursts and therefore was no longer in a favorable location to observe the incoming flow; rather, it observed compressions of the dipolar region as the flow bursts were braked tailward of the spacecraft. Increases in $B_z$ are correlated with the earthward flow perturbations, indicating that these were compressional signals.

The time shifts identified from the data indicate that the Pi2 signal appeared first at Geotail as velocity fluctuations ($t$=0), later as magnetic perturbations on the nightside at Isl and Lanl ($t$=+60 seconds), and finally as magnetic fluctuations on the dusk flank at Can and Lem ($t$=+92 seconds).

### 2.3. September 27, 1998

This third event occurred during extremely quiet geomagnetic conditions (Figure 1c). Geotail was located at (-9.9, 1.1, 0.6) in GSM coordinates. The mapped locations of the ground stations are shown in Figure 2c. The Geotail data (Figures 7a and 7b) show oscillations in the earthward component of the velocity starting at 2158 UT, followed by a slight dipolarization of the magnetic field. The spacecraft went into eclipse at 2206 UT. Polar VIS and UVI data indicate a localized arc brightening

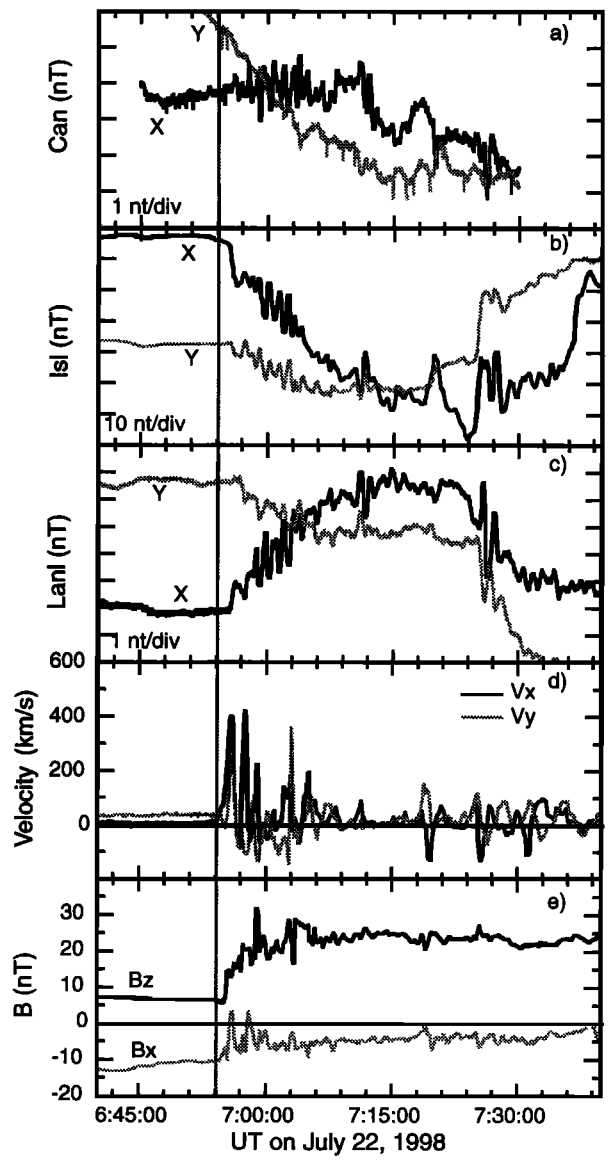


**Figure 4.** Geomagnetic field data from the (a) Canberra, (b) Island Lake (Isl), and (c) Los Alamos (Lanl) ground magnetometers for the July 22, 1998, event. (d) The X and Y components of the velocity from the Geotail spacecraft, in GSE coordinates. (e) Magnetic field data from the Geotail magnetometer in GSM coordinates.

between 2156:43 and 2201:13 UT. The ground data are shown in Figures 7c and 7d. Exact onsets of these Pi2 pulsations are difficult to determine, but it is clear that they begin around 2200 UT. The $V_x$ flow measured at Geotail and the ground magnetic field data (Figure 7f) correspond closely if the velocity data are shifted by +39 s. The individual flow bursts correspond to negative $Y$ and $Z$ perturbations at Crete. Similar oscillations are also seen at Lanl, Kat, and Jic. As in the September 4, 1997, event, the velocity variations are not exactly aligned with the ground Pi2. In particular, the +39 s shift is too large for the third burst (Figure 7f). The $V_y$ component for the first two bursts was positive, while for the third it was negative. In addition, the field became more dipolar during the event, and as we discuss in section 3.1., this may affect the propagation delay.

To identify propagation delays between ground stations, we have plotted in Figure 8 the sum of the squares of the envelopes of data from Kat and Crete filtered in the Pi2 band (40-150 s), which gives the total Pi2 power. The temporal variations of power is very similar at these two stations after ~2200 UT, with Kat delayed relative to Crete by ~30 s.

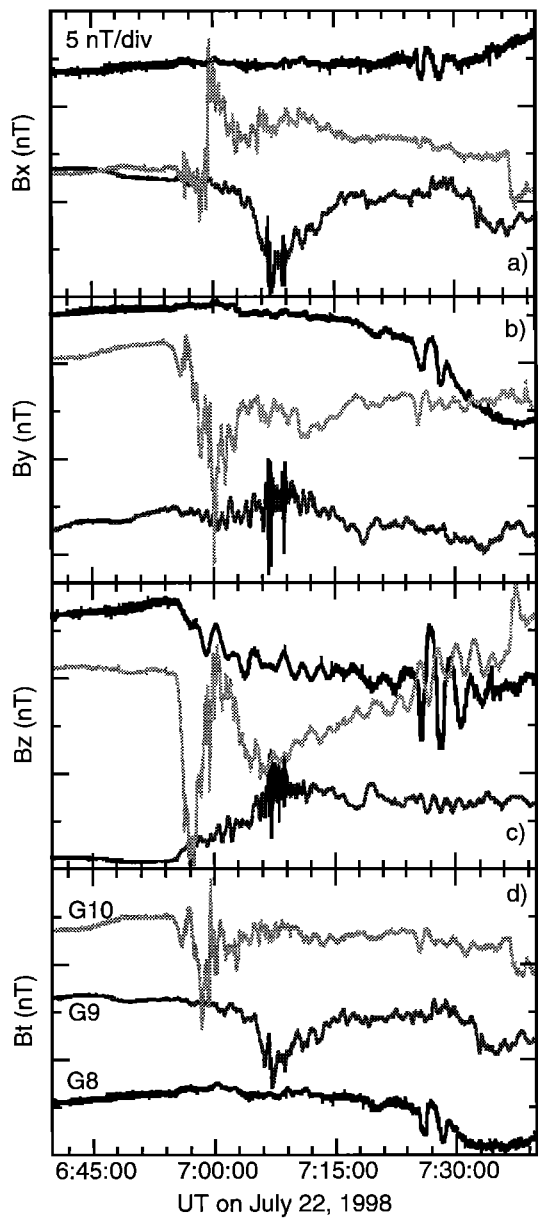


**Figure 5.** Magnetometer data from GOES 8 (black), GOES 9 (dark gray), and GOES 10 (light gray) for the July 22, 1998, event.

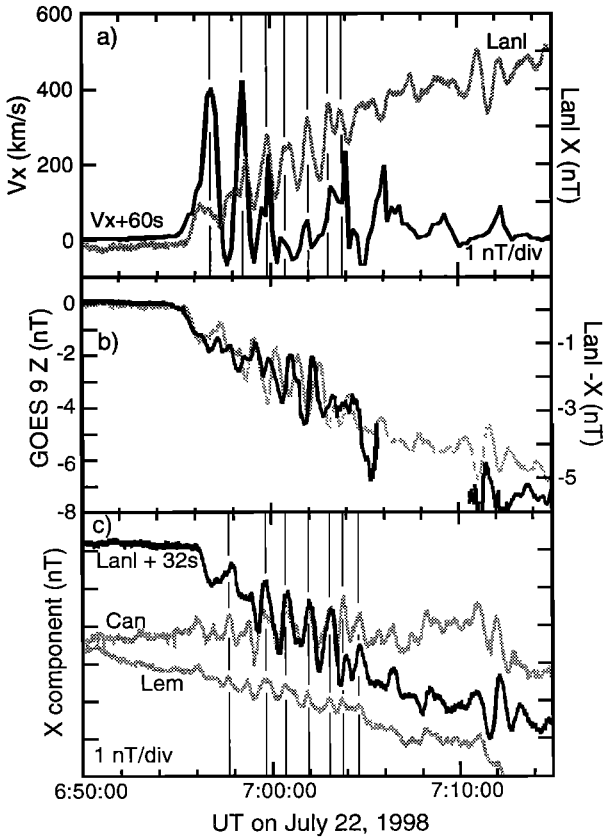


**Figure 6.** (a) Comparison of the $X$ component of the flow velocity from Geotail and the $X$ component of the magnetic field measured by the Los Alamos (Lanl) magnetometer. The Geotail data have been shifted by +60 s. (b) The -$X$ component of the magnetic field of the Lanl magnetometer (gray) and the $Z$ component of the magnetic field from GOES 9 (black). Data showing large-amplitude Pi1 pulsations ($T$ ~ 6 s) between 0706 and 0710 UT have been removed for clarity. (c) Comparison of ground magnetic field data from Los Alamos (-$X$ component), Canberra ($X$ component), and Learmonth ($X$ component). Los Alamos has had a +32 s shift applied.

### 2.4. July 18, 1996

The positions of the Geotail spacecraft and ground stations are shown in Figure 2d. The *CU* and *CL* indices show that this event occurred near the onset of a medium substorm, which peaked in intensity ~20 min later (Figure 1d). Polar VIS images show an auroral onset between 0658:58 and 0703:27 UT followed by poleward expansion consistent with a moderate substorm. An electron injection was observed by the 1990-095 geosynchronous satellite just after 0700 UT. Geotail was located at (-8.9, 4.8, -0.13) $R_E$ in GSM coordinates and measured a brief flow enhancement in the earthward component at ~0657:30 UT, followed by two more at 0700 and 0702 UT (Figures 9a and 9b). The third enhancement contained a large $V_y$ component.

Magnetic field data from Sim and Can are presented in Figures 9c and 9d. Also plotted is time-shifted velocity data from Geotail.

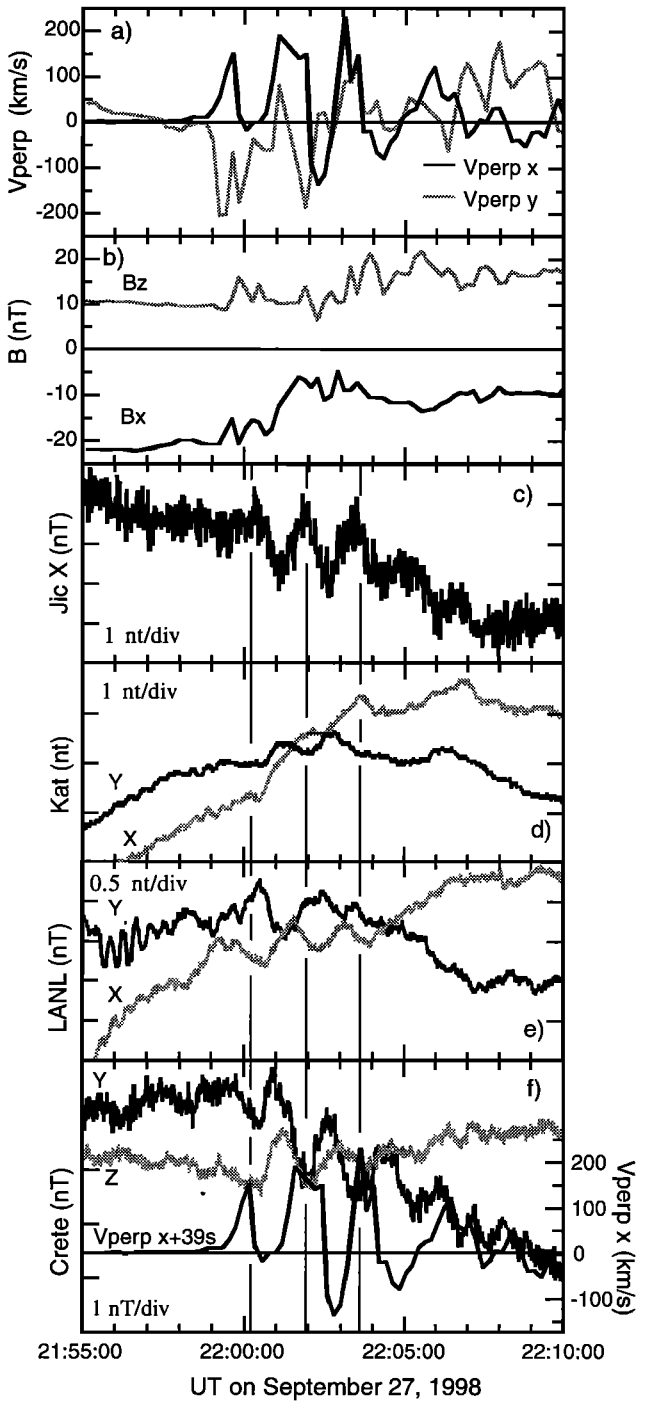


**Figure 7.** (a) The GSE perpendicular components of the ion velocity and (b) the GSM components of the magnetic field from Geotail for September 27, 1998. The spacecraft entered eclipse at 2206 UT. Also plotted are the ground magnetic field data from (c) Jicamarca (Jic), (d) Kataning (Kat), and (e) Los Alamos (Lanl). (f) A comparison of the variations in the earthward perpendicular velocity measured at Geotail and the $Y$ and $Z$ (vertical) components of the magnetic field measured at Crete. The Geotail data have been shifted by +39 s.

Sim observed negative $X$ perturbations at 0659, 0702:30, and 0703 UT, ~70 s after similar perturbations in the flow velocity were detected at Geotail. These perturbations were ~50 nT in amplitude, in the negative $X$ (southward) direction. Can, located at the dusk flank, observed similar perturbations an additional 40 s later, but with a much reduced amplitude (~1 nT).

### 2.5. October 26, 1997

The positions of the ground stations and Geotail are shown in Figure 2e. Geotail was located at (-13.6, 0.3, -1.2) $R_E$ in GSM coordinates. Polar UVI images indicate that this was a minor breakup. Auroral indices were not available, but Dawson of the Canopus magnetometer array was located near the breakup and showed a small negative bay (Figure 1e).

The magnetic field and particle data from Geotail are shown in Figures 10a and 10b. A large, variable, flow burst was observed starting at 1128 UT, which lasted for ~6 min. The magnetic field was highly variable during this period, and there was significant $B_z$ transport. Magnetic field data from the ground stations are shown in Figures 10c and 10d. The perpendicular components of the velocity measured at Geotail, shifted by +195 s, are shown in Figure 10e. The data from all three stations show Pi2 pulsations starting near 1132 UT, ~3 min after the start of the flow burst, with similar waveforms as the flow variations.

### 2.6. October 31, 1997

Geotail was located near midnight at (-15, -0.4 -0.1) $R_E$ in GSM coordinates (Figure 2f). Magnetic field and plasma data from the Geotail spacecraft are shown in Figure 11. A large flow enhancement began near 1741 UT and continued for ~5 min. The vertical component of the magnetic field increased from ~2 to ~10 nT, indicating that the field became more dipolar in this region. The horizontal components of the magnetic field from the ground stations Brv and Msr are shown in Figure 11c. These stations are nearly conjugate, with Msr located in the Northern Hemisphere. Four perturbations are evident, and they have been marked by vertical lines. The period between the first three perturbations is ~1 min, while the fourth occurs ~90 s after the third. Both stations observe negative $X$ perturbations, while the $Y$ perturbations are out of phase, consistent with an odd-mode perturbation. There is an initial small positive $X$ perturbation preceding the large negative deflections at 1743 and 1746:30 UT. The perpendicular components of the flow velocity measured at Geotail are shown in Figure 11d. Good agreement with the negative $X$ perturbations throughout the event is found if the flow data are shifted by +90 s.

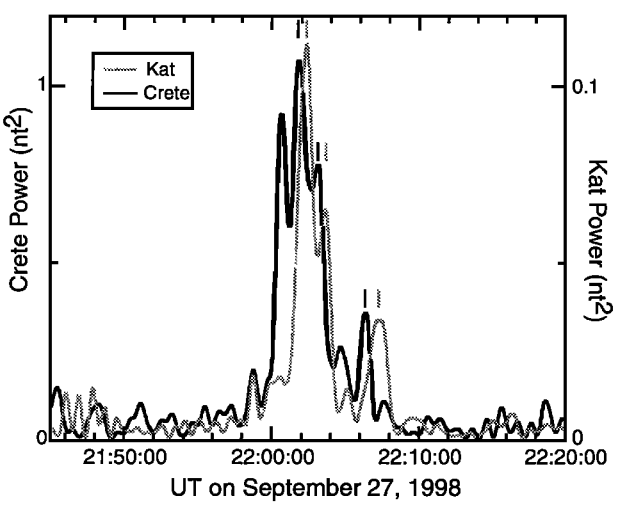


**Figure 8.** Sum of the squares of the envelopes of Pi2 filtered data for Crete and Kat.

## 3. Discussion

In the previous section we showed several events in which large earthward flows were observed in the near-Earth magnetotail near local midnight. The flow events were associated with varying degrees of dipolarization, auroral arc brightening, and electrojet intensification. Temporal modulations of the flow velocity measured in the near-Earth magnetotail by the Geotail spacecraft match Pi2 waveforms on the ground. Table 1 summarizes the delay between the Pi2 pulsations measured on the ground and the flow bursts in the magnetotail. In some instances an accurate delay time could not be determined.

As outlined in the introduction, Pi2 pulsations are categorized by the location where they are observed as midlatitude and low-latitude Pi2. This is an historical artifact that reflects the unknown source of the pulsations and often leads to confusion. Throughout the rest of this paper, we will abandon this nomenclature and instead adopt terminology relating to the underlying physics of the pulsations.

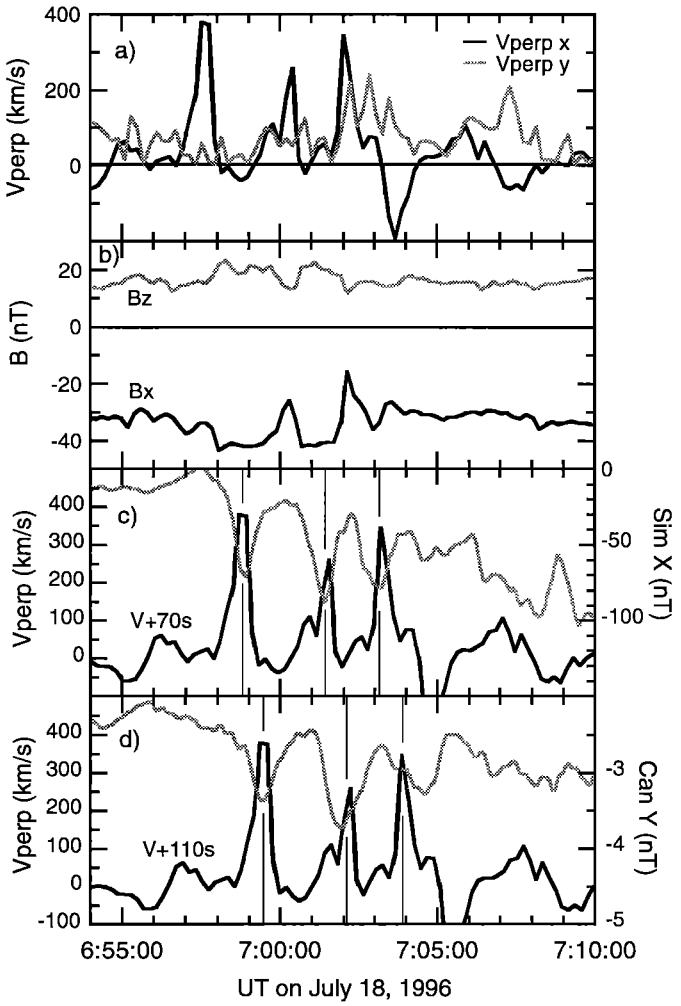


**Figure 9.** Data for the July 18, 1996, event. (a) The perpendicular components of the velocity and (b) the magnetic field measured at Geotail. (c) A comparison of the $X$ component from Sim and the earthward component of the perpendicular velocity observed at Geotail, shifted by +70 s. (d) A comparison of the $Y$ component from Can and the $X$ component of the perpendicular velocity, shifted by +110 s.

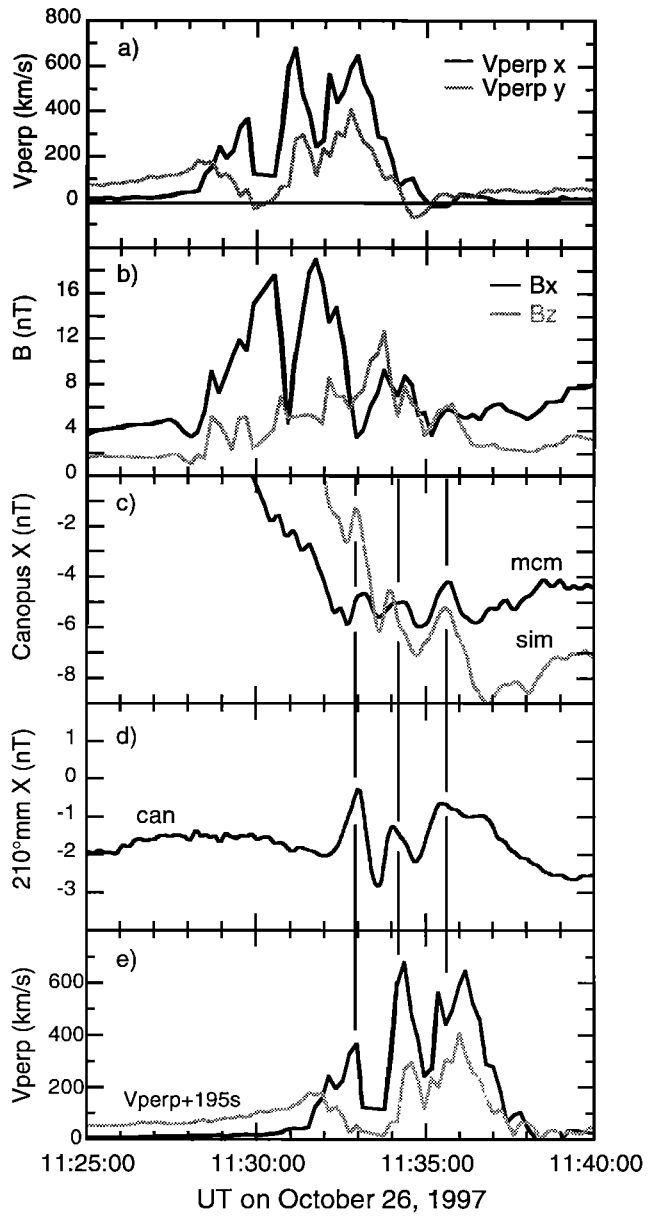


**Figure 10.** Data for the October 26, 1997, event. (a) The perpendicular velocity and (b) the magnetic field observed by Geotail. (c) The $X$ component of the magnetic field from Mcm and Sim. (d) The $X$ component from Can. (e) The $X$ and $Y$ components of the perpendicular velocity measured at Geotail, shifted by +195 s. Times when variations in the flow velocity match ground perturbations are marked with vertical lines.

Midlatitude Pi2 refer to nightside pulsations associated with the transient response of the substorm current wedge (SCW) as it establishes new flow patterns in the ionosphere. When referring to the general characteristics (such as polarization, amplitude profiles, etc.) of midlatitude Pi2 pulsations without specifying their underlying cause we will use the term SCW Pi2. We distinguish between two types of SCW pulsations, based on the mechanism that creates them. The first is created when an impedance mismatch between the ionosphere and magnetosphere exists. These Pi2 pulsations are well explained by the transient response model, and we will refer to them as transient response (TR) Pi2. We argue for a second, distinct class of Pi2s having the

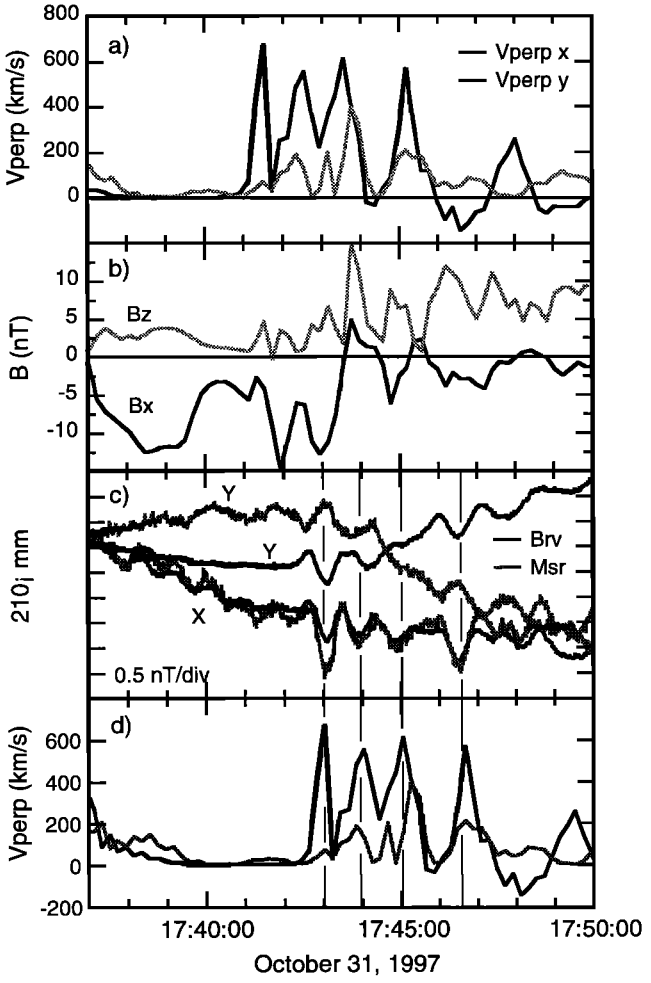


**Figure 11.** Data for the October 31, 1997, event. (a) The $X$ and $Y$ components of the perpendicular velocity and (b) the GSM magnetic field measured at Geotail. (c) The $X$ and $Y$ components of the magnetic field measured at Birdsville (Brv) and Moshiri (Msr). (d) The perpendicular velocity measured by Geotail, shifted by +90 s. Vertical lines mark times when positive (earthward) flow bursts match Pi2 perturbations at Brv and Msr.

same polarization and amplitude characteristics as the TR pulsations but arising from a different source mechanism that is directly related to transient flow braking. These we call inertial current (IC) Pi2 pulsations. Finally, we will argue that the low-latitude Pi2 presented in this paper are directly driven by flow variations, and hence we call these directly driven Pi2 pulsations. We present a simple model for propagation of fast-mode wave fronts from the flow-braking region to low-latitudes on the flank and dayside. Because we are uncertain as to whether it is the compressional or Alfvénic wave mode detected at low latitudes on the nightside, we do not discuss these Pi2 explicitly, though we feel the directly driven model can account for them.

### 3.1. Flank/Dayside Pi2

In a previous paper [*Kepko and Kivelson*, 1999], we reported on Pi2 pulsations observed on the flanks at low latitudes on the ground and in space outside the plasmasphere by two GOES spacecraft. These Pi2 pulsations were preceded by flows in the middle magnetotail with very similar waveforms. We concluded that these pulsations were most probably directly driven by the oscillatory flow observed on the nightside. The six events presented here support this conclusion. The relation of the flow modulation to the waveforms is again present in these additional events. Clearly, Geotail was located well outside the plasmasphere in all events and could not have been observing plasmaspheric oscillations.

Briefly, the braking of the periodic flow bursts generates compressional pulses that in turn, on the flanks and dayside, couple to Alfvén waves [see *Kepko and Kivelson*, 1999, Figure 11a]. On the nightside, ground stations may observe both a compressional and an Alfvénic component. The periodicity of the flow bursts establishes the Pi2 frequency at low latitudes. In one respect, the model is similar to the sudden commencement model of *Tamao* [1964]. There, an increase in solar wind dynamic pressure compresses the dayside magnetopause and launches a compressional wave tailward. If the wave is confined to the equatorial plane, Alfvén waves travel along field lines to the ionosphere. However, the two models differ in that the fast-mode wave of the SC model communicates the new compressed configuration of the magnetosphere to the flanks and nightside and leads to the formation of new large-scale field-aligned currents. In the directly driven Pi2 model the field lines at low latitudes are only momentarily displaced by the compressional pulse, and it is the pressure gradients created by dipolarization that create the current systems associated with convection. Note that it is not necessary for the flow to return to zero between bursts to generate Pi2. It is the relative rapid increase in the flow velocity that alters pressure balance at the tail/dipolar interface, and any sudden increase in flow velocity above the background will launch a compressional signal sunward.

Although we have applied a constant time shift to the flow data to compare with the ground magnetometer data, it is clear that in some cases a fixed time shift is not appropriate for an entire event (see, e.g, the September 4, 1997, and September 27, 1998, events). The delay to the ground stations is determined by the sum of the travel time of the flow to the braking region and of the fast-mode wave front sunward away from the braking region to the inner magnetosphere. The flows clearly are not constant in amplitude or direction and the location of the braking region moves tailward as flux is transported earthward. All of these effects alter the fraction of the distance over which the signal propagates at the fast-mode velocity as opposed to the bulk flow velocity. The delay from flow burst to ground Pi2 for the September 4, 1997, event seemed to depend greatly on the sign of $V_y$, as did the September 27, 1998, event. In both cases, when $V_y$ was in the direction of the stations the delay was smallest.

**Table 1.** Propagation Times for Each of the Three Events in this Paper, as Well as the Event From *Kepko and Kivelson [1999]*

| Event Date | Geotail $X$ ($R_E$) | Geotail Nightside, s | Nightside Flank/Dayside, s |
|---|---|---|---|
| 98/9/27 | -8.4 | +39 | +30 |
| 96/7/18 | -8.9 | +70 | +40 |
| 98/7/22 | -9.0 | +60 | +32 |
| 97/9/4 | -9.8 | +60 | — |
| 97/10/26 | -13.6 | +195 | — |
| 97/10/31 | -15 | +90 | — |
| 79/4/19 | -17.0 | +120 | +20 |

Read 98/9/27 as September 27, 1998.

We note that the delay for the July 22, 1998, event appears to be relatively constant, even though it has the longest duration and is therefore most likely to be affected by changes at the tail/dipolar interface. Geotail is in the dipolar region for this event, and the signal is propagating at the fast-mode velocity, which remains relatively constant earthward of Geotail. Therefore variations in the flow velocity or changes in the location of braking have no effect in determining the delay from Geotail to the ground.

As the fast-mode propagates sunward, it perturbs field lines and Alfvén waves propagated to the ionosphere. Several predictions follow from the directly driven scenario:

1. The pulsations should appear as odd-mode pulsations in the magnetic field. Accounting for a 90° ionospheric rotation [*Hughes*, 1974] (counterclockwise in the Northern Hemisphere, clockwise in the Southern Hemisphere) this predicts that magnetometers in opposite hemispheres would measure the $X$ component in phase and the $Y$ component out of phase. For all six events presented here all stations of the 210° mm observe the X component of the pulsations in phase, and although the Y component signal is sometimes very weak, opposite hemisphere stations recorded out of phase pulsations, consistent with an odd-mode structure.

2. Ignoring refraction of the equatorally confined fast-mode wave as it propagates through the inner magnetosphere, to first order the initial movement of the flux tube in the magnetosphere at the flanks should be sunward. This means that the initial Pi2 perturbation (assuming a 90° rotation through the ionosphere [*Hughes*, 1974]) at dusk on the ground should be northward, while at dawn it should be southward. Can, Dlb, and Ewa also observed an initial northward perturbation while located in the premidnight sector for the September 4, 1997, event. Because of the uncertainty in determining the onset of Pi2 in the data from September 27, 1998, the initial deflection on the flanks cannot be determined accurately, though it does appear as if Kat (on the dawn flank) observes an initial southward perturbation at 2200:30 UT. The ground data from the October 31, 1997, event in which 210° mm stations were located at ~0300 LT show negative X perturbations that are well correlated with the flow variations. However, they also show small positive perturbations just prior to these, suggesting that our model of an equatorally confined fast mode wave coupling to Alfvén waves is too simplistic. There may be a mixture of modes at these local times and latitudes. It is important to note that the largest-amplitude perturbations (and the ones that are most likely to be directly driven) are in the direction predicted. An extension of this prediction is that concurrent pulsations on opposite flanks will be 180° out of phase. We have only 1 event for which we have simultaneous opposite flank magnetometer data, but uncertainty in Pi2 onset times precludes cross-phase analysis. Some previous work has reported opposite polarizations at the two flanks [e.g., *Sutcliffe*, 1981].

### 3.2. Substorm Current Wedge (SCW) Pi2: Transient Response and Inertial Current Pi2

Many properties of nightside Pi2 pulsations are well organized by the geometry of the substorm current wedge. Pi2 amplitude is largest in the auroral zone, near the equatorward edge of the westward electrojet current that closes the substorm current wedge through the ionosphere [*Jacobs and Sinno*, 1960; *Rostoker and Samson*, 1981; *Samson*, 1982]. *Lester et al.* [1983] found that in most Pi2 events, the principal axis of polarization of nightside Pi2 pulsations across a latitudinal array of magnetometers points toward the center of the current wedge. It was later determined that midlatitude Pi2 are produced by oscillations of field-aligned current on the SCW [*Hughes and Singer*, 1985] and the principal axis points toward the head of the westward traveling surge [*Gelpi et al.*, 1987]. In space, the initial deflection is in the direction expected for the field-aligned current system [*Sakurai and McPherron*, 1983]. Finally, the $H$ component perturbations are in phase over a range of latitudes, while the $D$ component perturbations are out of phase in opposite hemispheres [*Yumoto et al.*, 1994], consistent with the direction of perturbations expected from the substorm current wedge.

The description of high-latitude and midlatitude Pi2 pulsations as bouncing Alfvén waves associated with the diversion of cross-tail current into the substorm current wedge is called the transient response model (for a review, see *Baumjohann and Glassmeier* [1984]). If an Alfvén wave with electric perturbation $E_0$ is incident on the ionosphere, the reflected electric field $E_r$ is

$$E_r = \frac{2E_0}{1+\Sigma_P/\Sigma_A} - E_0, \tag{1}$$

where $\Sigma_P$ is the height-integrated Pedersen conductivity in the ionosphere and $\Sigma_A = 1/\mu_0 v_A$ is the wave conductivity with $v_A$ the Alfvén speed. If the conductivities $\Sigma_P$ and $\Sigma_A$ are equal, then (1) shows that the reflected electric field vanishes, but more typically, $\Sigma_P/\Sigma_A$ is large, and the reflected field is $\sim -E_0$. The Pedersen conductivity changes with local time, latitude, and magnetic activity and thus is likely to control wave reflection. Low conductivity, as might be expected on the nightside during quiet periods, produces little reflection, so Pi2 are not generated by this transient response mechanism. Nightside conductivity increases during active times as particles precipitate into the ionosphere. This increases wave reflection and the bouncing waves generate transient response (TR) Pi2 pulsations. The periods are determined by wave travel times along the flux tube.

The field-aligned current ($j_\parallel$) that forms the substorm current wedge is fed by a diversion of the perpendicular current ($\mathbf{j}_\perp$),

$$\mathbf{j}_\perp = \frac{\mathbf{B}}{B^2} \times \rho \frac{d\mathbf{u}}{dt} + \frac{\mathbf{B}}{B^2} \times \nabla P, \tag{2}$$

where $\rho$ is the number density, $\mathbf{B}$ is the magnetic field, $P$ is the thermal pressure, and $\mathbf{u}$ is velocity. In order to understand the generation of TR-Pi2s, it is useful to distinguish clearly the contributions of the two terms in (2). The first term on the right-hand side (RHS) (which we define as $j_{inrt}$) is the inertial current. It arises from the acceleration of a flow burst and is transient, being present only while flows are changing or are sheared. Once the flow has decelerated, both the inertial current and the perturbation field associated with it disappear. The second term on the RHS (which we define as $j_{\nabla p}$) provides the dominant parallel current in substorms. This current arises from the magnetic stresses and thermal pressure gradients generated by the dipolarization and flow diversion [*Birn et al.*, 1999]. Even after the plasma flows stop, this current may remain finite. It is responsible for releasing accumulated stresses in the magnetosphere and driving most of the current of the substorm current wedge [*Birn et al.*, 1999].

We now describe qualitatively the events that generate Pi2s at midlatitudes on the nightside and their effects as measured by a ground station. As a flow burst nears the inner magnetosphere it is braked, creating the inertial current that flows dusk to dawn in the magnetosphere. This current is diverted along magnetic field lines at the edges of the flow channel into the ionosphere creating the SCW. Simultaneously, magnetic shears and thermal pressure

gradients near the braking region are increased. The enhanced currents, $j_{inrt}$ and $j_{\nabla p}$, together form the SCW, and are to first order collocated with each other.

In Figure 12 we show idealized examples of mid-latitude signatures that occur as a result of an oscillatory flow burst of the type observed by Geotail and presented in this paper. They illustrate the ground signatures of the current systems described above. We first show the perturbations due to a traditional substorm current wedge system, accounting for contributions arising from $j_{\nabla p}$ only, with no reflection of the incoming Alfvén wave, and no braking current, $j_{inrt}$ (Figure 12a). This produces a positive bay at midlatitudes where the magnetic perturbations are imposed by the field-aligned portion of the SCW and there are no Pi2s. If we include reflection (i.e., an impedance mismatch between the magnetosphere and ionosphere), the traditional midlatitude Pi2 (which we term TR Pi2) riding a positive bay is generated as illustrated by the transient response model (Figure 12b). Note that the sinusoidal oscillations continue even after the flow has stopped. They decay as the magnetosphere and ionosphere approach equilibrium and disappear when the maximum perturbation is reached. The $j_{\nabla p}$ currents and the flow bursts operate over different timescales. The flows last just a few minutes while the $j_{\nabla p}$ currents flow for the duration of the substorm.

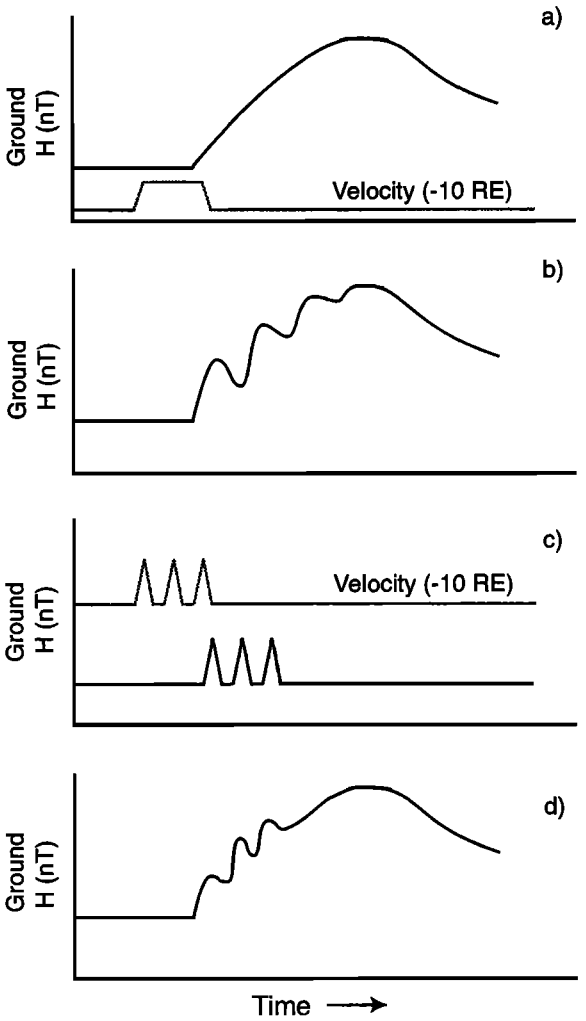


**Figure 12.** Qualitative plots of perturbations measured by nightside, midlatitude ground stations under a variety of conditions. (a) A traditional substorm current wedge system, with no reflection of incoming waves and no inertial current. (b) same as Figure 12a with reflection, which leads to the generation of transient response (TR) Pi2 pulsations. (c) Ground perturbations (which we term IC Pi2) due to time varying inertial current, without the substorm current wedge. (d) A substorm current wedge without reflection, but including the inertial current.

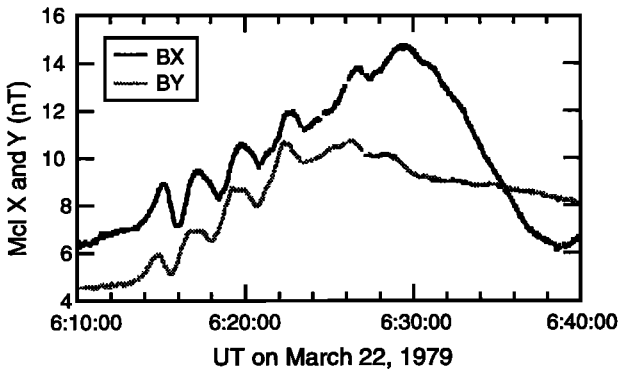


**Figure 13.** Example of a midlatitude, transient response (TR) Pi2 signature. The Mount Clemens (Mcl) magnetometer was located at 55.8° CGM latitude and was at ~2300 MLT at this time.

If we ignore contributions to the substorm current wedge current from $j_{\nabla p}$ and consider instead just the response to the time-varying braking current $j_{inrt}$, a ground station will observe perturbations due to the pulses of braking-generated current, with no additional change in the background field (Figure 12c). The positive bay driven by pressure gradients would not develop in this case. If a $j_{\nabla p}$ is also present but the incoming wave does not reflect from the ionosphere (i.e., no impedance mismatch), oscillations of the sort illustrated in (Figure 12c) will modify a midlatitude positive bay (Figure 12d), but the properties of these oscillations will differ from those shown in (Figure 12b). Importantly, the oscillations are not damped sinusoids. Their amplitude remains relatively constant, unlike TR Pi2, and they disappear when the flows stop.

A good example of the TR Pi2 is shown in Figure 13. It shows the damped, sinusoidal waveform expected from the transient response model (compare with Figure 12b). The nightside Pi2s observed on July 22, 1998, between 0655 and 0706 UT exhibit the polarization characteristics, amplitude profile, and initial deflection expected for the TR Pi2, but they differ from this type because the waveforms match the flow variations in the magnetotail (Figure 6). The July 18, 1996 (Figure 9c), and October 26, 1997 (Figure 10c), events show the same characteristics. This correlation between midtail plasma flow and midlatitude magnetic perturbation cannot be explained by the transient response model. The Pi2 periods are not those of bouncing Alfvén waves; rather, the periods correspond to the time variation of the flows. The perturbations stop when the flow stops, in contrast to pulsations generated by the transient response model. These Pi2 also differ from the directly driven pulsations previously discussed in section 3.1. in that their initial perturbations are systematically linked to the substorm current wedge. For example, the initial deflection changes between Island Lake (which measured perturbations due to the ionospheric segment of the SCW) and Los Alamos (which responded to the field-aligned portions of the SCW), both on the midnight meridian at different $L$ values. The different perturbations would not arise in the directly driven model unless nodes occur in the radial direction, which seems improbable.

The currents associated with the inertial process of flow braking are expected to flow along the substorm current wedge and can explain the Pi2 observed on July 22, 1998, July 18, 1996, and October 26, 1997. We call these Pi2 "inertial current" Pi2, or IC Pi2. Their characteristics are similar to those of the TR Pi2, yet they arise from different sources, and the periods are determined by very different mechanisms.

In most Pi2 events the frequency, and hence waveforms, differ for nightside midlatitude (SCW) Pi2 and for low-latitude flank and dayside Pi2s [see, e.g., *Stuart and Barsczus*, 1980]. In a previous study [*Kepko and Kivelson*, 1999], we showed an event in which low-latitude flank Pi2 correlated well with flow variations measured by the ISEE 2 spacecraft, located on the nightside in the middle magnetotail, while nightside mid-latitude stations concurrently observed a longer period pulsation not directly associated with the flow variations. We argue that in these cases the flank Pi2s are directly driven by flow variations in the magnetotail, while the nightside Pi2s are generated by the reflection of the incoming current of the substorm current wedge, whose frequency is imposed by the properties of the tail flux tubes and is independent of the flow variations. We have termed these TR Pi2. Because the $j_{\nabla p}$ current is a factor of 10-100 times larger than the inertial current [*Birn et al.*, 1999], typical amplitudes of the TR Pi 2 (10-20 nT) are much larger than the amplitudes arising from the inertial current (1-2 nT). When both are present, the TR Pi2 dominate the signatures making it appear that the inertial current system is not active. Spectral evidence suggests that both pulsations may be present on the nightside. *Li et al.* [1998] find that high-latitude pulsations show two spectral peaks, with peak power at the lower frequency. We argue that this shows that both pulsations are present and that the relative amplitudes reflect the dominance of TR Pi2 over IC Pi2. Lower-latitude stations on the nightside showed the same two spectral peaks, yet the higher-frequency component dominated there. Low-latitude stations lie far from the substorm current wedge, and the directly driven waves are likely to dominate.

We now must address the events of July 22, 1998, July 18, 1996, and October 26, 1997, in which the IC Pi2 is clearly evident but the TR Pi2 is not (see Figure 4c). According to (1) the incoming Alfvén wave associated with the switching on of the substorm current wedge current will not reflect from the ionosphere if the ionospheric conductivity is low. We note that magnetospheric activity was quite low before two of these events, and nightside ionospheric conductivity may have been exceptionally low. We suggest that a priming of the nightside ionosphere must occur before TR Pi2 are observed.

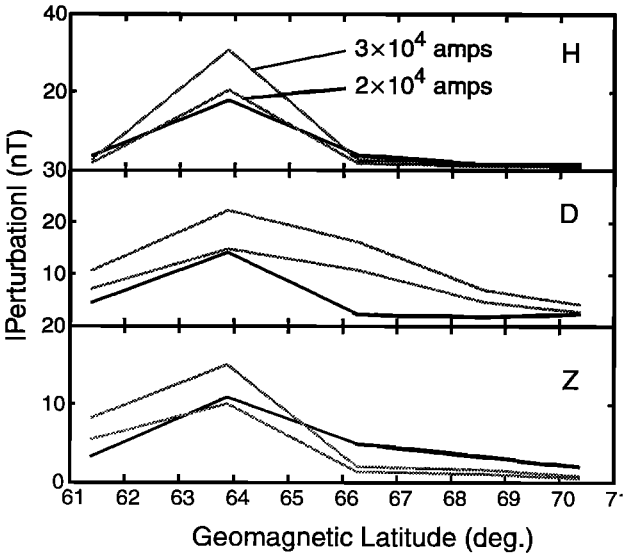


**Figure 14.** Measurements of the inertial current for the July 22, 1998, event. The black lines are measurements from the Canopus magnetometers, and gray lines are model fits.

### 3.3. Estimate of the Braking Current

We argued in section 3.2 that nightside stations observed perturbations (IC Pi2 pulsations) arising from the braking current flowing along the substorm current wedge for the July 22, 1998, event. Let us next calculate the magnitude of this current and compare with values calculated from the measured flow in the

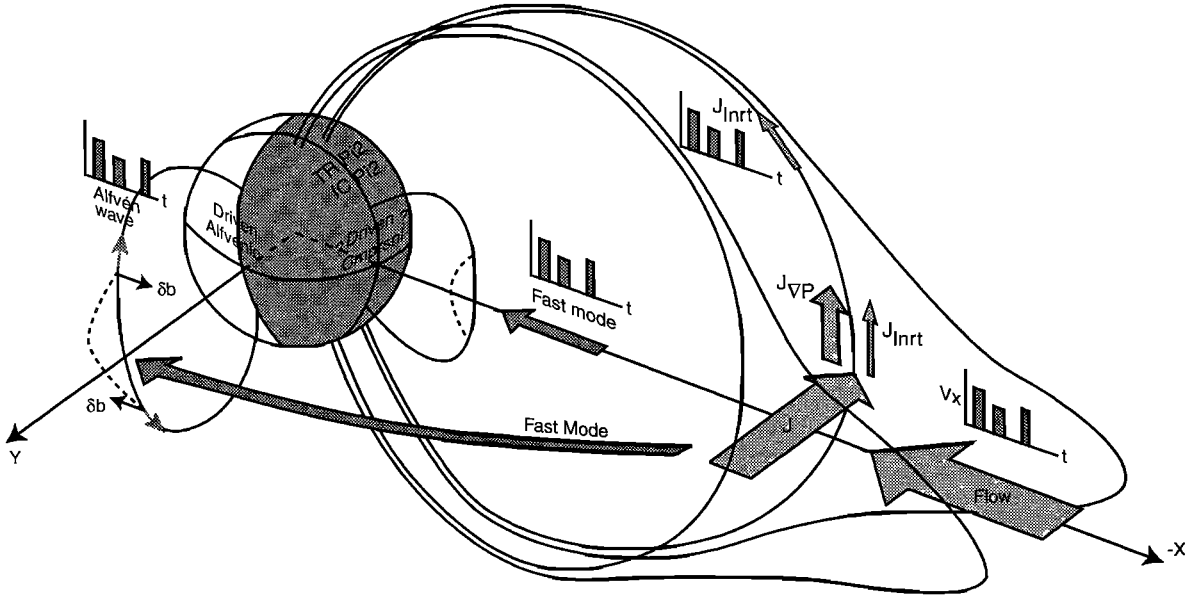


**Figure 15.** Summary of Pi2 generation (see text for details).

magnetosphere. Figure 14 shows a profile of the maximum perturbation from the IC Pi2 pulsations observed along the Fort Churchill chain of magnetometers from the Canopus magnetometer array between 0656 and 0703 UT. We calculated the effect of a substorm current wedge using a line current model and the Biot-Savart law. The footprints of the SCW were placed at 64.5°N latitude with a 30° width centered on the Fort Churchill chain (336° CGM longitude). The current was assumed to flow along dipole field lines. The results, shown as gray lines in Figure 14, indicate that a current between 2 and $3\times10^4$ amps produces magnetic perturbations that agree well with the observations.

The braking current ($I_{braking}$) in the plasma sheet is given by the first term on the RHS of (2). Expanding this term and setting the braking length over the timescale of braking, $L_x/\delta t$, to $1/2u_x$ gives [see *Haerendel*, 1992]

$$I_{braking} \cong -\frac{1}{4}B_{ps}^{-1}\rho_{ps}u_x^2 l \qquad (3)$$

where the *ps* refers to plasma sheet properties and $l$ is the scale height of braking. Using the values measured for this event by Geotail ($n_{ps}$ = 1 cm$^{-3}$, $B_{ps}$ = 20 nT, $u_x$ = 500 km/s), and assuming a vertical scale height of $l$ = 2 $R_E$ we find $I_y \cong 6\times10^4$ A. This value is an upper limit to the current to which ground stations respond, since some of the current may not be directed into the ionosphere. Despite this caveat we note that this value is of the same order as the value calculated above from the ground perturbations. We performed similar calculations for the July 18, 1996, event and obtained a current of $I_y \cong 3\times10^4$ A flowing in the ionosphere. Since Geotail was not in the braking region for this event, we cannot calculate the braking current using (3). For comparison, *Shiokawa et al.* [1997] obtained $10^5$ A for the breaking current using Geotail observations, and *Birn et al.* [1999] obtained $3\times10^5$ A from an MHD simulation. A typical substorm current wedge contains ~$10^6$ A.

## 4. Conclusions

We have examined six events in which the Geotail spacecraft observed periodic flow enhancements near the braking region. All six preceded Pi2 pulsations with similar waveforms on the ground by ~1-3 min. We believe that these observations combined with the wide body of previous research on Pi2 pulsations are consistent with the following scenario (summarized in Figure 15):

1. A bursty bulk flow with flow enhancement hits the dipolar inner magnetosphere, launching an equatorally confined compressional pulse. The antisunward flow bursts repeat quasiperiodically.

2. As each compressional pulse travels antisunward, it perturbs field lines, thus producing a single Pi2 impulse on the ground. A series of compressional pulses produces a Pi2 train, and the waveforms of these pulsations match the waveforms of the flow bursts in the magnetotail. We term these "directly driven Pi2." Stations on the flank observe Alfvénic perturbations, and we suggest that stations on the nightside at low latitudes may observe compressional perturbations, though more work is required before a definitive statement can be made.

3. As a flow burst is decelerated or braked at the tail/dipolar transition region a transient current flows from dusk to dawn in the equatorial region. Closure currents flow toward and away from the ionosphere in the auroral zone and contribute to the substorm current wedge. We refer to this transient current as the inertial current system. These currents flow only while the flow is decelerating. The process drives Pi2 pulsations localized to the nightside with polarization parallel to the substorm current wedge perturbations, including the phase reversal at midlatitudes. The waveforms of these Pi2 match the waveforms of the flow bursts. We call these inertial current (IC) Pi2s.

4. An additional, larger contribution to the current of the substorm current wedge, driven by pressure gradients and flow shears, extends over larger distances in $y$ and $x$ and flows longer (tens of minutes to an hour) than the inertial currents. If an impedance mismatch between the ionosphere and magnetosphere exists, the leading edge of this current system is reflected. This sets up a Pi2 with the period determined by the flux tube bounce time, typically longer than the period of flow variation. These Pi2, which we have termed transient response (TR) Pi2, do not match the waveform of the flow bursts (not shown in Figure 15).

**Acknowledgments.** *AE* indices were provided by the Kyoto WDC. Polar VIS and UVI images were obtained from CDAWeb and were provided by L. Frank and G. Parks, respectively. The CANOPUS instrument array was constructed and is maintained and operated by the Canadian Space Agency. GEOTAIL magnetic field data and plasma data were provided by S. Kokubun and T. Mukai through DARTS at the Institute of Space and Astronautical Science (ISAS) in Japan. Additional ground data were provided by V. Angelopoulos (Lanl and Crete magnetometers) and D. Sibeck (Jic) and were obtained from the UCLA data server at http://www-ssc.igpp.ucla.edu/uclamag/data_center/. We acknowledge H. Singer for providing and assisting in our interpretation of the GOES magnetometer data. This work was supported by the National Science Foundation under grants ATM 93-14239 and ATM 98-20106 and the Los Alamos Division of the Institute of Geophysics and Planetary Physics, UCRP 708. Institute of Geophysics and Planetary Physics publication #5473.

Janet G. Luhmann thanks Kazue Takahashi and Peter R. Sutcliffe for their assistance in evaluating this paper.

## References

Angelopoulos, V., C. F. Kennel, F. V. Coroniti, R. Pellat, M. G. Kivelson, R. J. Walker, C. T. Russell, W. Baumjohann, W. C. Feldman, and J. T. Gosling, Statistical characteristics of bursty bulk flow events, *J. Geophys. Res.*, *99*, 21,257, 1994.

Baumjohann, W., and K.-H. Glassmeier, The transient response mechanism and Pi2 pulsations at substorm onset — Review and outlook, *Planet. Space Sci.*, *32*, 1361, 1984.

Baumjohann, W., G. Paschmann, and H. Lühr, Characteristics of high-speed ion flows in the plasma sheet, *J. Geophys. Res.*, *95*, 3801, 1990.

Birn, J., and M. Hesse, Details of current disruption and diversion in simulations of magnetotail dynamics, *J. Geophys. Res.*, *101*, 15,345, 1996.

Birn, J., M. Hesse, G. Haerendel, W. Baumjohann, and K. Shiokawa, Flow braking and the substorm current wedge, *J. Geophys. Res.*, *104*, 19,895, 1999.

Gelpi, C., H. J. Singer, and W. J. Hughes, A comparison of magnetic signatures and DMSP auroral images at substorm onset: Three case studies, *J. Geophys. Res.*, *92*, 2447,1987.

Goertz, C. K., and R. W. Boswell, Magnetosphere-ionosphere coupling, *J. Geophys. Res.*, *84*, 7239, 1979.

Haerendel, G., Disruption, ballooning or auroral avalanche — On the cause of substorms, *Proc. of the International Conference on Substorms (ICS-1)*, pp. 417-420, ESA Publications Division, Noordwijk, The Netherlands,1992.

Hughes, W. J., The effect of the atmosphere and ionosphere on long period magnetospheric micropulsations, *Planet. Space Sci.*, *22*, 1157, 1974.

Hughes, W. J., and H. Singer, Mid-latitude Pi2 pulsations, geosynchronous substorm onset signatures and auroral zone currents on march 22, 1979: CDAW 6, *J. Geophys. Res.*, *90*, 1297, 1985.

Jacobs, J. A., and K. Sinno, World-wide characteristics of geomagnetic micropulsations, *Geophys. J.*, *3*, 333, 1960.

Kepko, E. L., and M. G. Kivelson, Generation of Pi2 pulsations by bursty bulk flows, *J. Geophys. Res.*, *104*, 25,021, 1999.

Kokubun, S., T. Yamamoto, M. H. Acuna, K. Hayashi, K. Shiokawa, and H. Kawano, The GEOTAIL Magnetic Field Experiment, *J. Geomagn. Geoelectr.*, *46*, 7-21, 1994.

Lester, M., W. J. Hughes, and H. Singer, Polarization patterns of Pi2

magnetic pulsations and the substorm current wedge, *J. Geophys. Res.*, *88*, 7958, 1983.

Li, Y., B. J. Fraser, F. W. Menk, D. J. Webster, and K. Yumoto, Properties and sources of low and very low latitude Pi2 pulsations, *J. Geophys. Res.*, *103*, 2343, 1998.

Lysak, R. L., and C. T. Dum, Dynamics of magnetosphere-ionosphere coupling including turbulent transport, J. *Geophys. Res.*, *88*, 365, 1983.

Maltsev, Y. P., W. B. Lyatsky, and A. M. Lyatskaya, Currents over the auroral arc, *Planet. Space Sci.*, *25*, 53, 1977.

Mallinckrodt, A. J., and C. W. Carlson, Relations between transverse electric fields and field-aligned currents, *J. Geophys. Res.*, *83*, 1426, 1978.

McPherron, R. L., Magnetospheric substorms, *Rev. Geophys.*, *17*, 657, 1973.

Mukai, T , S. Machida, Y. Saito, M. Hirahara, T Terasawa, N. Kaya, T. Obara, M. Ejiri, and A Nishida, The Low Energy Particle (LEP) Experiment onboard the GEOTAIL satellite, *J Geomagn. Geoelectr.*, *46*, 669-692, 1994.

Nagai, T., M. Fujimoto, Y. Saito, S Machida, T. Terasawa, R. Nakamura, T. Yamamoto, T. Mukai, A. Nishida, and S. Kokubun, Structure and dynamics of magnetic reconnection for substorm onsets with geotail observations, *J. Geophys. Res.*, *103*, 4419, 1998

Nishida, A., Possible origin of transient dusk-to-dawn electric field in the nightside magnetosphere, *J Geophys. Res.*, *84*, 3409, 1979

Olson, J , Pi2 pulsations and substorm onsets. A review, *J. Geophys Res.*, *104*, 17,499, 1999.

Rostoker, G., and J. C. Samson, Polarization characteristics of Pi2 pulsations and implications for their source mechanisms: Location of source regions with respect to the auroral electrojets, *Planet. Space Sci* , *29*, 225, 1981.

Saito, T., Geomagnetic pulsations, *Space Sci. Rev.*, *10*, 319, 1969.

Saito, T., T. Sakurai, and Y. Koyama, Mechanism of association between Pi2 pulsation and magnetospheric substorm, J. *Atmos Terr Phys* , *38*, 1265, 1976.

Sakurai, T , and R L. McPherron, Satellite observations of Pi2 activity at synchronous orbit, *J. Geophys Res.*, *88*, 7015, 1983.

Sakurai, T., and T. Saito, Magnetic pulsation Pi2 and substorm onset, *Planet. Space Sci* , *24*, 573, 1976

Samson, J. C., Pi2 pulsations· High latitude results, *Planet Space Sci.*, *30*, 1239, 1982.

Shiokawa, K., W. Baumjohann, and G. Haerendel, Braking of high-speed flows in the near-Earth tail, *Geophys. Res. Lett.*, *24*, 1179, 1997.

Southwood, D. J., and W. J. Hughes, Concerning the structure of Pi2 pulsations, *J. Geophys. Res.*, *90*, 386, 1985.

Stuart, W. F., and H. Barsczus, Pi's observed in the daylight hemisphere at low latitudes, *J. Atmos. Terr. Phys.*, *42*, 487, 1980.

Sutcliffe, P. R., Ellipticity variations in Pi2 pulsations at low-latitudes, *Geophys. Res. Lett.*, *8*, 91, 1981.

Sutcliffe, P. R , and K. Yumoto, Dayside Pi 2 pulsations at low latitudes, *Geophys. Res. Lett.*, *16*, 887, 1989

Sutcliffe, P. R., and K. Yumoto, On the cavity mode nature of low-latitude Pi2 pulsations, *J. Geophys. Res.*, *96*, 1543, 1991.

Tamao, T., Hydromagnetic interpretation of geomagnetic SSC, *Rep. Ionos. Space Res. J.*, *18*, 16, 1964.

Yeoman, T. K., and D. Orr, Phase and spectral power of mid-latitude Pi2 pulsations: Evidence for a plasmaspheric cavity resonance, *Planet. Space Sci* , *37*, 1367, 1989

Yumoto, K., and the 210° MM Magnetic Observation Group, The STEP 210° magnetic meridian network project, *J Geomagn. Geoelectr* , *48*, 1297, 1996

Yumoto, K , K. Takahashi, T Saito, F. W. Menk, B J Fraser, T. A. Potemra, and L. J Zanetti, Some aspects of the relation between Pi 1-2 magnetic pulsations observed at $L$ = 1 3-2.1 on the ground and substorm-associated magnetic field variations in the near-Earth magnetotail observed by AMPTE CCE, *J. Geophys. Res.*, *94*, 3611, 1989.

Yumoto, K., H. Osaki, K. Fukao, K. Shiokawa, Y. Tanaka, S. I. Solovyev, G. Krymsku, E. F. Vershinin, V F. Osinin, and 210 MM Magnetic Observatory Group, Correlation of high- and low-latitude Pi2 magnetic pulsations observed at 210 magnetic meridian chain stations, *J. Geomagn. Geoelectr.*, *46*, 925, 1994.

L. Kepko and M. G. Kivelson, Department of Earth and Space Sciences, 405 Hilgard Avenue, Los Angeles, CA 90095-1567. (lkepko@igpp.ucla.edu)

K Yumoto, Department of Earth and Planetary Physics, Kyushu University, Fukuoka 812-8581, Japan.

(Received April 25, 2000; revised August 7, 2000,
accepted August 22, 2000 )